Shortened version of the title:

Fatigue of T300/924 Composites with Voids

Full title:

Fatigue Characterization of T300/924 Polymer Composites with Voids Under Tension-tension and Compression-compression Cyclic Loading

Authors:

Hao-long Liu[1], Hai-tao Cui[1, 2], Wei-dong Wen[1, 2], Hong-tae Kang[3]

Affiliations:

[1]College of Energy and Power Engineering, Nanjing University of Aeronautics and Astronautics, Nanjing, China

[2]State Key Laboratory of Mechanics and Control of Mechanical Structures, Nanjing University of Aeronautics and Astronautics, Nanjing, China

[3]College of Engineering and Computer Science, University of Michigan-Dearborn, Dearborn, MI, USA

Corresponding author:

Haolong Liu, Nanjing University of Aeronautics and Astronautics, 29 Yudao St., Nanjing 210016, China.

Email: haolongl@umich.edu

This is the author manuscript accepted for publication and has undergone full peer review but has not been through the copyediting, typesetting, pagination and proofreading process, which may lead to differences between this version and the Version of Record. Please cite this article as doi: 10.1111/ffe.12721

Fatigue Characterization of T300/924 Polymer Composites with Voids Under Tension-tension and Compression-compression Cyclic Loading

Hao-long Liu[1], Hai-tao Cui[1, 2], Wei-dong Wen[1, 2], Hong-tae Kang[3]

[1]College of Energy and Power Engineering, Nanjing University of Aeronautics and Astronautics, Nanjing, China

[2]State Key Laboratory of Mechanics and Control of Mechanical Structures, Nanjing University of Aeronautics and Astronautics, Nanjing, China

[3]College of Engineering and Computer Science, University of Michigan-Dearborn, Dearborn, MI, USA

Abstract

Fibrous polymer composites exhibit excellent properties such as high specific stiffness/strength and good fatigue performance. However, as inherent defects of polymer composites, voids have been reported to have an impact on their load-bearing properties including fatigue resistance. In the interest of safety, the effect of voids on fatigue behaviors of composites should be understood and quantified. In this article, effect of voids on the fatigue of T300/924 composites was evaluated in terms of their fatigue life, stiffness degradation, and cracks propagation under tension-tension and compression-compression loadings. The failure probability was assessed by Weibull distribution. Furthermore, crack measurement and fractographic analysis reveal that the effect of voids on the failure mechanisms of the material under various loading configurations could be different. Lastly, an analytical residual stiffness model was proposed, and a good correlation was obtained between the experimental data and the prediction results.

Keywords: polymer composite; effect of voids; fatigue behaviors; crack density measurement.

1. Introduction

For the last decades, a growing interest has been seen in extensive use of carbon fiber reinforced polymer (CFRP) composites in a wide range of manufacturing industries. As low weight has become one of the most urgent targets for both vehicles and airplanes in meeting customer demands and government regulations for energy efficiency, the situation can be improved with the implementation of CFRP composites because of their many advantages in terms of high strength-to-density ratio and

good fatigue resistance. Vast amount of works have been done to investigate the mechanical properties of polymer composites; however, some of the work revealed that the voids have an impact on the mechanical properties, especially fatigue performance [1–10].

It has been commonly accepted that the fatigue process of composites is totally different and more complicated compared with that of metals. The complexity derives from different failure mechanisms, which are influenced by several factors according to previous studies: (1) mechanical properties of the material components, such as fiber, matrix, and fiber-matrix interface [11]; (2) fiber orientation and fiber volume fraction [12, 13]; and (3) manufacturing defects and material aging due to the extreme working conditions (e. g., fiber defects [14], voids [1–10], and mechanical degradation due to hygrothermal aging [15] or ultraviolet radiation [16]). Among these factors, voids, as one of the most common defects in resin polymer composites, are inevitably induced during manufacturing process. Many researchers devoted to investigating the formation mechanisms of voids [17, 18], the effect of voids on the quasi-static properties [19–21] and the fatigue properties of composites [1–10].

As early as 1981, the effect of voids on composite structures has drawn attentions of researchers. Garbo and Ogonowski [1] investigated the effect of voids on the fatigue of composite joints, they stated that up to moderate porosity, the presence of voids has limited effect on the fatigue life of the joint. In the same year, R. Prakash [2] studied fatigue fracture surfaces of HM-S/828 composite using a scanning electron microscope, a failure hypothesis for composites with the presence of defects (voids, etc.) was put forward based on the fractographic evidences. Since then, the effects of voids on fatigue behaviors of composite materials were studied by researchers across the world [3–10]. de Almeida [3] investigated the effect of voids on the flexural fatigue of AS4/PMR-15 composite, a strong detrimental effect on the fatigue performance of the composite structure was observed when the void content was above a critical value. J. Lambert [4] characterized the voids and their distribution in a glass fiber reinforced polymer composite used in wind turbine blades, the fatigue mechanisms were also examined using computed tomography (CT). M.A. Suhot and A.R. Chambers [5, 6] explored the effect of voids on the flexural fatigue properties of unidirectional carbon fiber polymer composites used in the wind turbine industry, they reported a general trend of increasing fatigue strength with decreasing porosity level. Sanjay Sisodia [7] investigated the effect of voids on

the quasi-static and tension-tension fatigue properties of HTS40/RTM6 laminated composite, the results showed that the fatigue life of the composite was sensitive to the void content. Apart from the studies on the effect of voids alone, studies on fatigue behaviors of composites with void defect in certain environment have also been reported. A.Y. Zhang [10] investigated the effect of voids on the bending strength and bending fatigue of T300/914 laminated composite exposed to hygrothermal environment, they found that both the bending strength and bending fatigue performance of the material decreased with increasing level of porosity.

This study focuses on the characterization of the effect of voids on the tension-tension (T-T) and compression-compression (C-C) fatigue of CFRP laminated composites. The characterization of voids was accomplished first, and the fatigue properties of composites were studied through the following aspects: (1) fatigue life, fatigue strength, and failure probability distribution of laminated composites; (2) residual stiffness degradation on the basis of the change of the hysteresis loop in the course of fatigue; (3) failure mechanisms based on the observation of crack initiation/propagation and SEM fractographic analysis; and (4) analytical fatigue model with regard to the residual stiffness. We expect that the present investigation could be helpful in understanding the effect of voids on the fatigue of fibrous polymer laminated composites under different loading configurations, and could serve as a guide line in the safety design in engineering applications.

2. Experimental

2.1 Materials

T300/924 laminated composite, as a commonly used CFRP composite, was fabricated and tested in this study. To control the void content in the epoxy matrix, different compression pressures (0.5MPa, 0.3MPa, and 0.1MPa) were chosen in compression molding. The temperature in curing process first increases with a heating rate of 6℃/min, and levels off at 180℃ for two hours before cooling down. The stacking sequences of the plaques consist of $[0]_{12}$, $[0]_{16}$, $[90]_{12}$ and $[0/\pm45/0/90]_s$. The thickness of a single ply is approximately 0.14mm. A digital microscopy image module was proposed in this study to examine the void content, morphology of voids, and the fiber volume fraction (The detailed curing process, manufacturing parameters, and properties of the fibers and the matrix can be found in Fig. S1, Table S1, and Table S2 in Supplementary Information).

2.2 Porosity Characterization

The samples for porosity characterization, with dimensions of 10mm×10mm, were cut from the composite plaques using a water jet. These samples were first embedded in epoxy resin and cured for 24 hours; the cross sections were then prepared by abrasive papers and synthetic diamond compounds. To obtain clear micro-images of the samples, an optical microscope with a CMOS camera connected to a computer was used in this article. For the purpose of providing a statistically representative data set, 5 samples were prepared for each plaque, and 3 images per sample were examined. To reduce the system error, the positions of samples on the plaques were randomly selected. Some typical micro-images of the samples cured at different compression pressures are shown in Fig. 1.

2.3 Testing configuration

In accordance with ASTM D3039, rectangular samples with various geometries were used in this study. To protect the gripping section, glass fiber reinforced polymer (GFRP) composite tabs were attached to both ends of the samples. The tabs were attached to the samples by epoxy adhesive 3M^{TM} DP420, which is capable of providing adequate shear strength after being cured at 150℃ for 15 hours according to our test results. Specific fixtures were manufactured to hold the tabs in position and to provide essential pressure when the adhesive was cured in the oven. The preparation and configurations of samples are shown in Fig. 2.

All the tests were conducted in an MTS 647 hydraulic servo dynamic testing machine, and the configurations of the tests are shown in Fig. 3. The quasi-static tensile tests and compression tests were performed under displacement control with displacement rate equaled 1mm/min, while the fatigue tests were performed under load control. In the tensile tests, 5 samples were tested for laminate with given lay-up and void content. The axial strain was captured by an extensometer (MTS E 634.31F-24) (the detailed quasi-static tensile test data can be found in Table S4 in Supplementary Information). To avoid the impact of high temperature as a result of the high loading frequency and high loading level in fatigue tests, temperature measurement for short rectangular specimens was conducted to determine a proper loading frequency. A thermal camera, as shown in Fig. 3 (b) to (d), was used to monitor the temperature change on the surface of the sample, assisted by a pyrometer as

validation. The temperature of the sample would increase at the beginning of the test and reach a steady state after certain number of cycles. In this article, the steady state temperatures (SST) at different loading frequencies and loading levels were recorded, and iso-temperature-rise curves were drawn (Fig. 3 (e)). According to the test results, a frequency of 7Hz was selected to avoid high temperature as well as to guarantee an acceptable test speed. The load ratio R=0.1 was used in the T-T fatigue tests and R=10 in C-C fatigue tests. The Young's modulus degradation of the sample was traced with the help of the evolution of secant slope of the hysteresis loop.

In addition, to investigate the effect of voids on the fatigue deterioration of the composite under T-T fatigue loading, transverse crack density evolution was studied by measuring the crack density at both lateral surfaces of the specimen. In this study, the evolution of crack density was examined based on optical micro-images by interrupting the fatigue tests at certain stages.

3. Results and Discussions

3.1 Voids characterization

Samples from plaques cured at various compression pressures were examined to determine the void content. Table 1 presents the resulting averaged void content of each plaque. The detailed void content measurement results can be found in Table S3 and Fig. S2 in Supplementary Information.

Fig. 4 (a) to (c) demonstrate the distribution of aspect ratio versus the equivalent diameter of voids in 12-ply UD plaques cured under 0.5MPa, 0.3MPa, and 0.1MPa, respectively. It is clear that for all three plaques, most of the points lie on the right side of the dashed line, which suggests that smaller voids tend to be closer to spherical. According to Fig. 1, the interlaminar voids, which usually derive from the entrapped air during autoclaving, are usually larger in size and have a higher average aspect ratio compared to intralaminar voids, which usually come from the volatiles that derive from the chemical reactions during the manufacturing process. These larger and more irregular voids may play a crucial role to accelerate the initiation and propagation of cracks when subjected to cyclic loading.

3.2 Fatigue life assessment

T-T fatigue tests were performed for UD composites in longitudinal/transverse direction and for MD laminates with a stacking sequence of $[0/\pm 45/0/90]_s$, while C-C tests were performed for UD

laminates in longitudinal direction. The specimens were subjected to different stress levels corresponding to various fractions of ultimate tensile strength (UTS) or compression stress (UCS). For both the UD and the MD laminates, failure of specimen was programmed in the test machine as complete fracture. However, the failure of the MD specimens is different as compared to that of the UD specimens. To be specific, for the longitudinal UD laminates, no obvious damage could be seen prior to fracture. Specimens split suddenly at final failure, with numerous debris burst out; due to vast amount of delamination and fiber-matrix interfacial de-bonding, no clear fracture surfaces could be observed. Whereas for the MD specimens, large amount of inter-ply failures could be seen before final failure. Besides, plies with different fiber orientations have different failure modes: for 0º plies, fiber breakage and interfacial de-bonding are the dominant failure modes; whereas for ±45º and 90º plies, cracks propagate along the fiber orientation, and severe inter-fiber-bundle failures and fiber/matrix interfacial de-bonding can be observed.

The effect of voids on the fatigue behaviors of the composite was first assessed in terms of fatigue life. Fig. 5 (a) and (b) depict the S-N diagrams for T-T fatigue tests of UD laminates in longitudinal and transverse directions, respectively. The fatigue life decreases almost linearly as the stress level increases. It is evidently clear that for the UD laminated composites, increase of void content would always lead to decrease of fatigue life when subjected to T-T cyclic loading. Meanwhile, a lower fatigue strength can be found for materials with higher porosity level as well, both for longitudinal and transverse directions. In addition, the transverse fatigue resistance is more sensitive to the porosity level (Fig. 5 (b)). Given the dominant failure mode in the transverse test is matrix cracking rather than fiber breakage, it is reasonable to assume that the presence of voids has a more significant impact on the matrix-dominated mechanical properties of the fibrous composites.

Similar effect of voids can be observed for MD laminates with a stacking sequence of $[0/\pm45/0/90]_s$ subjected to T-T fatigue loading and UD laminates subjected to C-C loading, where the S-N curve seems to experience a translational displacement as the porosity level increases (Fig. 5 (c) and (d)). However, the C-C fatigue of UD laminates seems to be more sensitive to the stress level compared with the T-T fatigue (detailed experimental data of the fatigue tests are presented in Table S5 to Table S8 in Supplementary Information). Finally, tests for poolability showed that the

individual data sets in each figure cannot be pooled.

In an attempt to evaluate the fatigue discreteness of the laminated composites and to assess the durability of the material in terms of the failure probability, a two-parameter Weibull distribution function was used in this study (Eq. (1) in Appendix A). Fig. 6 (a) to (d) present the failure probabilities and the predictive results for UD laminates under longitudinal/transverse T-T fatigue loading, MD laminates under T-T fatigue loading, and UD laminates under longitudinal C-C fatigue loading, respectively. The fitting parameters can be found in Table 2. A good correlation can be observed between the failure probability and the number of cycles.

By plotting the test data on the mean stress-stress amplitude plane, a constant fatigue life diagram for UD laminate was drawn to take both the effect of voids and effect of mean stress into account (Fig. 7). The fatigue life at certain stress level, porosity level, and stress ratio was obtained by interpolation based on a simple $S - N_f$ fatigue model (Eq. (3) in Appendix A).

3.3 Stiffness degradation

The fatigue damage of composites can be evaluated in terms of the degradation of macroscopically measurable properties such as residual stiffness or strength. Compared to residual strength, the usage of residual stiffness as a detector of the damage induced by the cyclic loading has advantages due to its non-destructive nature and smaller scatter. In this study, the dynamic stiffness degradations of samples subjected to T-T fatigue loadings were analyzed through the same method described in literature [22]. The degradation of residual modulus was extracted on the basis of the secant slope of the line segment between the maximum of minimum points of each cycle (Fig. 8 (a)). Fig. 8 (b) and (c) show the hysteresis loops at certain cycles for UD composites subjected to fatigue loadings in the longitudinal and transverse directions, respectively. Obvious translational displacement and rotation of the hysteresis loop can be observed as the number of cycles increases.

In Fig. 9 (a) and (b) are presented the normalized stiffness degradations of UD laminates subjected to longitudinal and transverse cyclic loading, respectively. As shown in the figures, higher stress levels are accompanied by faster stiffness reduction processes (e. g., for laminates with void content of 0.8%, the sample tested at stress level of 82% experienced a more rapid axial modulus decrease with respect to the number of cycles as compared with that of samples tested at stress levels

of 75% and 68%). Moreover, higher load levels corresponding to a larger decrease in moduli were also observed, which is consistent with the analytical results of Gowayed [23] based on shear lag theory.

The evaluations of effect of voids for laminates subjected to given stress levels are presented in Fig. 9 (c) and (d). According to the figure, the presence of voids is able to significantly accelerate the fatigue damage accumulation process in both cases. As void content increases, the axial modulus decreases more rapidly up to fracture occurs, thus leading to a shorter fatigue life. However, the modulus drop for laminates with different void contents at rupture seems not to be affected by the presence of voids, as shown in Fig. 9 (d).

For the purpose of quantitatively assessing the effect of voids on the fatigue behaviors of composites and to provide a method to predict the fatigue life of components during components design, a simple predictive method was deduced on the basis of the stiffness degradation of composites at various porosity levels (Eq. (6) in Appendix A). By using quadratic polynomial equations, the functions δ, φ_1, and φ_2 can be well fitted with the correlation coefficients ranging from 0.926 to 0.971. The results pertaining to the fitting curves are presented in Fig. 10. A good correlation can be observed between the test data and the fitting results.

3.4 Damage evaluation through crack density measurement

For composites subjected to T-T fatigue loading, stiffness variation can be attributed to matrix cracking. To explain the effect of voids on the fatigue mechanisms of composites under T-T loading, matrix cracks on the free edges of the UD laminates were assessed at specified cycles using an optical microscope. Fig. 11 (a) shows the microscopic images of matrix cracks at various stages of the fatigue, while Fig. 11 (b) shows the evolution of matrix crack density for laminates at various stress levels and porosity levels. According to Fig. 11 (a), matrix cracks are apt to nucleate from interlaminar voids and propagate into the ply, indicating a faster crack initiation/propagation. The results are consistent to the crack density measurement results shown in Fig. 11 (b). For laminates with higher void content, matrix cracks would reach saturation state in fewer cycles. However, the saturation of matrix cracks seems not to be associated with the porosity level. To conclude, the presence of voids would accelerate the fatigue of CFRP composites by stimulating the evolution of

matrix cracks.

3.5 Fatigue fractographic analysis

Aside from the crack density measurement during the course of fatigue, the fractographic analysis was also performed as a supplemental approach to further reveal the effect of voids on the fatigue failure mechanisms of composites. The post-failure modes and facture morphology of the longitudinal UD specimens with various void contents are shown in Fig. 12. Intriguingly, although the presence of voids, as shown in the previous section, would shorten the fatigue life of composites by stimulating the matrix cracks to nucleate and propagate, specimens with 0.8% and 4% voids share similar features of fractures. Large amount of delamination (Fig. 12 (a)), fiber pull-outs, broken fibers, and matrix plastic deformation (Fig. 12 (c, e)) can be observed. However, subtle differences can still be found in meso-scale SEM images of the fracture surfaces. Owing to a higher level of porosity, matrix cracks in laminates with higher void content may tend to deflect into fiber orientation to form fiber-matrix interface damage, thereby resulting in "rougher" crack surfaces (Fig. 12 (b, d)).

Despite specimens with different void contents share fairly similar characteristics for T-T fatigue fracture surfaces; in C-C fatigue tests, a clear discrepancy can be observed in fracture morphology of laminates at various porosity levels (Fig. 13). Relative flat fracture surfaces were found for specimens with void content of 0.8% (Fig. 13 (b)), whereas "brush-like" fracture surfaces were observed for specimens with void content of 4% (Fig. 13 (a)). The "brush-like" feature can be attributed to vast amount of inter-fiber-bundle failure including delamination owing to the presence of voids. As discovered in the previous study, the voids, as inherent defects of the material, could stimulate the matrix crack in the material when subjected to T-T fatigue loading. Similarly, inter-phase failure may tend to initiate from the voids as well under C-C cyclic loading, the formation of fiber-matrix interface failure and delamination could trigger the unstable failure of fibers at early stage of fatigue, thus leading to fewer cycles to failure. Although there was also delamination occurred in composites with lower void content (Fig. 13 (d, e)), the fracture surfaces were relatively flat, with an angle formed (approximately 51°, Fig. 13 (c)) with respect to the fiber direction.

4. Conclusions

By performing the fatigue testing and the relative analysis for T300/924 laminated composites at various porosity levels, this work successfully evaluated the effects of voids on their tension-tension and compression-compression fatigue behaviors, alongside the initiation/propagation of matrix cracks and fatigue failure mechanisms. The fatigue behaviors of the composite displayed a high dependency on the void content when subjected to both T-T and C-C loading. The relationship between applied stress level and the corresponding fatigue life was correlated by a semi-logarithmic linear model, with the slope and intercept of the fitted curves described as functions of void content to capture the voids-induced effects. Apart from fatigue life, the effect of voids showed different mechanisms for T-T and C-C fatigue failure of the composite. To be specific, for specimens under T-T cyclic loading, revealed by the matrix crack density measurement results, the presence of voids could stimulate matrix cracks to initiate and propagate, resulting in more rapid damage accumulation and stiffness reduction process. Whereas for specimens under C-C cyclic loading, voids seem to play a different role in fatigue of composites. By stimulating failures including the inter-phase failure and delamination to occur, the presence of voids would lead to earlier unstable fiber fracture as well as fewer cycles to failure. Lastly, a residual stiffness model and a probability failure model were established from the engineering perspective. The results of the work provided a comprehensive insight for fatigue behaviors of CFRP laminated composites under the influence of voids. The understanding of the effect of voids along with the related numerical models, which have taken the effect of voids into account, will be useful for the future engineering applications of laminated polymer composites with voids defects.

Appendix A. Appendix

A.1. $p-S-N_f$ Model

The Weibull distribution used in this article is shown in Eq. (1), in which the two parameters $\eta(u)$ and $\lambda(u)$ represent the scale and shape parameters, respectively. Here the stress level u is defined as the ratio of the maximum stress and the UTS (in T-T tests) or UCS (in C-C tests).

$$P(n_i) = 1 - exp(-\left(\frac{n_i}{\eta(u)}\right)^{\lambda(u)}) \quad (1)$$

In this equation, i stands for the serial number of the sample, and $P(n_i)$ is the failure

probability of the No. i sample. The scale and shape parameters can be obtained by transforming Eq. (1) into the following equation.

$$ln(n_i) = \frac{1}{\lambda} ln\big(-ln\big(1 - P(n_i)\big)\big) + ln(\eta) \tag{2}$$

The parameters can then be obtained through linear regression on the basis of the test data.

A.2. $S - N_f$ Model

The $S - N_f$ model used in this article was based on the model proposed by Shokrich [24, 25] and Harris [26]. As shown in the S-N diagram, translational displacement and rotation can be observed in the S-N curve for laminates at different porosity levels. To take the effect of voids into account, the constants in the conventional model are replaced by the function of void content. The modified expression is as shown in Eq. (3).

$$u' = \frac{ln(a/f)}{ln[(1-q)(c+q)]} = \gamma(v_v) + k(v_v) lg N_f \tag{3}$$

In this equation, $a = (\sigma_{max} - \sigma_{min})/2[\sigma_t]$, $q = (\sigma_{max} + \sigma_{min})/2[\sigma_t]$, $c = [\sigma_c]/[\sigma_t]$, $[\sigma_t]$ is the tensile strength, $[\sigma_c]$ is the compression strength. f is a constant. $\gamma(v_v)$ and $k(v_v)$ are functions of v_v. $\gamma(v_v)$ is the intercept of the S-N curve with the vertical axis, while $k(v_v)$ is the slope of S-N curve.

A.3. Residual stiffness model

The fatigue damage of composites was assessed by a damage index based on the stiffness variations in previous research [27, 28] (Eq. (4)).

$$D = \frac{E_0 - E(N)}{E_0 - E(N_f)} \tag{4}$$

In this equation, E_0 indicates the initial modulus without damage, $E(N)$ indicates the residual modulus of the N^{th} cycle, N_f is the fatigue life.

H. Mao [29] proposed a classic residual stiffness model for fibrous composites, as shown in Eq. (5), the model well reflected the three-stage characteristic of the stiffness degradation in the course of fatigue process. In the equation, q, m_1, and m_2 are independent parameters ($m_1 < 1$, $m_2 > 1$). The first term in the equation captures the rapid stiffness reduction at the beginning, while the second term describes the damage accumulation at the end of the fatigue process.

$$D = q\left(\frac{n}{N_f}\right)^{m_1} + (1-q)\left(\frac{n}{N_f}\right)^{m_2} \quad (5)$$

Here, for the purpose of capturing the effect of voids, the shape parameters were further defined as functions of void content and stress level (Eq. (6)).

$$D = A\delta(u, v_v)\left(\frac{N}{N_f}\right)^{\varphi_1(u,v_v)} + (1 - A\delta(u, v_v))\left(\frac{N}{N_f}\right)^{\varphi_2(u,v_v)} \quad (6)$$

In this equation, A is a constant associated with the material. δ, φ_1, and φ_2 are functions of u and v_v. The expression of the functions can be obtained through curve fitting of the stiffness degradation data from the tests. Actually, the fatigue life can be straightly predicted by Eq. (7) once the relative residual stiffness is measured.

$$\frac{E(N)}{E_0} = 1 - \left(1 - \frac{E(N_f)}{E_0}\right)\left[A\delta(u, v_v)\left(\frac{N}{N_f}\right)^{\varphi_1(u,v_v)} + (1 - A\delta_1(u, v_v))\left(\frac{N}{N_f}\right)^{\varphi_2(u,v_v)}\right] \quad (7)$$

Appendix B. Supplementary document

The supplementary material associated with this article can be found in the Supplementary Information.

References

[1] Garbo, S.P.; Ogonowski, J.M. Effect of variances and manufacturing tolerances on the design strength and life of mechanically fastened composite joints. AFWAL-TR-81-3041 1981, vol. 1.

[2] Prakash, R. Significance of defects in the fatigue failure of carbon fibre reinforced plastics. FIBRE SCI TECHNOL 1981, 14, 171–181.

[3] de Almeida, S.F.M.; Neto, Z.S.N. Effect of void content on the strength of composite laminates. COMPOS STRUCT 1994, 28 (2), 139–148.

[4] Lambert, J.; Chambers, A. R.; Sinclair, I.; Spearing, S. M. 3D Damage Characterization and the Role of Voids in the Fatigue of Wind Turbine Blade Materials. COMPOS SCI TECHNOL 2012, 72 (2), 337–343.

[5] Suhot, M.A.; Chambers, A.R., The effect of voids on the flexural fatigue performance of unidirectional carbon fibre composites. 16th Int Conference on Composite Materials, Kyoto, Japan, 2007.

[6] Chambers, A.R.; Earl, J.S.; Squires, C.A.; Suhot, M.A. The effect of voids on the flexural fatigue performance of unidirectional carbon fibre composites developed for wind turbine applications. INT J FATIGUE 2006, 28, 1389–1398.

[7] Sisodia, S.; Gamstedt, E.K.; Edgren, F.; Varna, J. Effects of voids on quasi-static and tension fatigue behaviour of carbon-fibre composite laminates. J COMPOS MATER 2014, 0 (0), 1–12.

[8] Protz, R.; Kosmann, N.; Gude, M.; Hufenbach, W.; Schulte, K.; Fiedler, B. Voids and their effect on the strain rate dependent material properties and fatigue behaviour of non-crimp fabric composites materials. COMPOS PART B-ENG 2015, 83, 346–351.

[9] Schmidt, F.; Rheinfurth, M.; Horst, P.; Busse, G. Multiaxial fatigue behaviour of GFRP with evenly distributed or accumulated voids monitored by various NDT methodologies. INT J FATIGUE 2012, 43, 207–216.

[10] Zhang, A.Y.; Li, D.H.; Lu, H.B.; Zhang, D.X. Qualitative separation of the effect of voids on the bending fatigue performance of hygrothermal conditioned carbon/epoxy composites. MATER DESIGN 2011, 32, 4803–4809.

[11] Bathias, C. An engineering point of view about fatigue of polymer matrix composite materials. INT J FATIGUE 2006, 28, 1094–1099.

[12] Song, J.; Wen, W.D.; Cui, H.T.; Liu, H.L.; Xu, Y. Effects of temperature and fiber volume fraction on mechanical properties of T300/QY8911-IV composites. J REINF PLAST COMP 2014, 34 (2), 157–172.

[13] Allah, M.H.; Abdin, E.M.; Selmy, A.I.; Khashaba, U.A. Effect of fibre volume fraction on the fatigue behaviour of GRP pultruded rod composites. COMPOS SCI TECHNOL 1996, 56 (1), 23–29.

[14] Huang, X.S. Fabrication and Properties of Carbon Fibers. MATERIALS 2009, 2, 2369–2403.

[15] Hu, Y.H.; Lang, A.W.; Li, X.C.; Nutt; S.R. Hygrothermal aging effects on fatigue of glass fiber/polydicyclopentadiene composites. POLYM DEGRAD STABIL 2014, 110, 464–472.

[16] Zhang, J.Y.; Sun, C.Q.; Zhao, L.B.; Fei, B.J. Experiment Research of Environment Effects on Fatigue Life of Carbon/Bismaleimide Composite Laminates with Central Hole. KEY ENG MATER 2011, 452-453, 525–528.

[17] Liu, L.; Zhang, B.M.; Wang D.F.; Wu, Z.J. Effects of cure cycles on void content and

mechanical properties of composite laminates. COMPOS STRUCT 2006, 73, 303–309.

[18] Koushyar, H.; Alavi-Soltani, S.; Minaie, B.; Violette, M. Effects of variation in autoclave pressure, temperature, and vacuum-application time on porosity and mechanical properties of a carbon fiber/epoxy composite. J COMPOS MATER 2011, 46 (16), 1985–2004.

[19] Liebig, W.V.; Viets, C.; Schulte, K.; Fiedler, B. Influence of voids on the compressive failure behaviour of fibrereinforced composites. COMPOS SCI TECHNOL 2015, 117, 225–233.

[20] Selmi, A. Void Effect on Carbon Fiber Epoxy Composites. 2nd International Conference on Emerging Trends in Engineering and Technology (ICETET'2014), London, May 30-31, 2014.

[21] Costa, M.L.; Almeida, S.M. The influence of porosity on the interlaminar shear strength of carbon/epoxy and carbon/bismaleimide fabric laminates. COMPOS SCI TECHNOL 2001, 61, 2101–2108.

[22] Bensadoun, F.; Vallons, K.A.M.; Lessard, L.B.; Verpoest, I.; Van Vuure, A.W. Fatigue behavior assessment of flax–epoxy composites. COMPOS A APPL SCI MANUF 2016, 82, 253–66.

[23] Gowayed, Y.; Ojard, G.; Santhosh, U.; Jefferson, G. Modeling of crack density in ceramic matrix composites. J COMPOS MATER 2015, 49 (18), 2285–2294.

[24] Shokrieh, M.M.; Lessard, L.B. Progressive Fatigue Damage Modeling of Composite Materials, Part I: Modeling. J COMPOS MATER 2000, 34, 1056–1080.

[25] Shokrieh, M.M.; Lessard, L.B. Progressive Fatigue Damage Modeling of Composite Materials, Part II: Material Characterization and Model Verification. J COMPOS MATER 2000, 34, 1081–1116.

[26] Harris, B.; Gathercole, N.; Lee, J.A.; Reiter, H.; Adam, T. Life-prediction for constant-stress fatigue in carbon-fibre composites. Phil. Trans. R. Soc. Lond. A 1997, 355, 1259–1294.

[27] Reifsnider, K. Fatigue behavior of composite materials. INT J FRACTURE 1980, 16 (6), 563–583.

[28] Jamison, R.D. Advanced Fatigue Damage Development in Graphite Epoxy Laminates. Defense Technical Information Center: Fort Belvoir, VA, 1982.

[29] Mao, H.; Mahadevan, S. Fatigue damage modelling of composite materials. COMPOS STRUCT 2002, 58, 405–10.

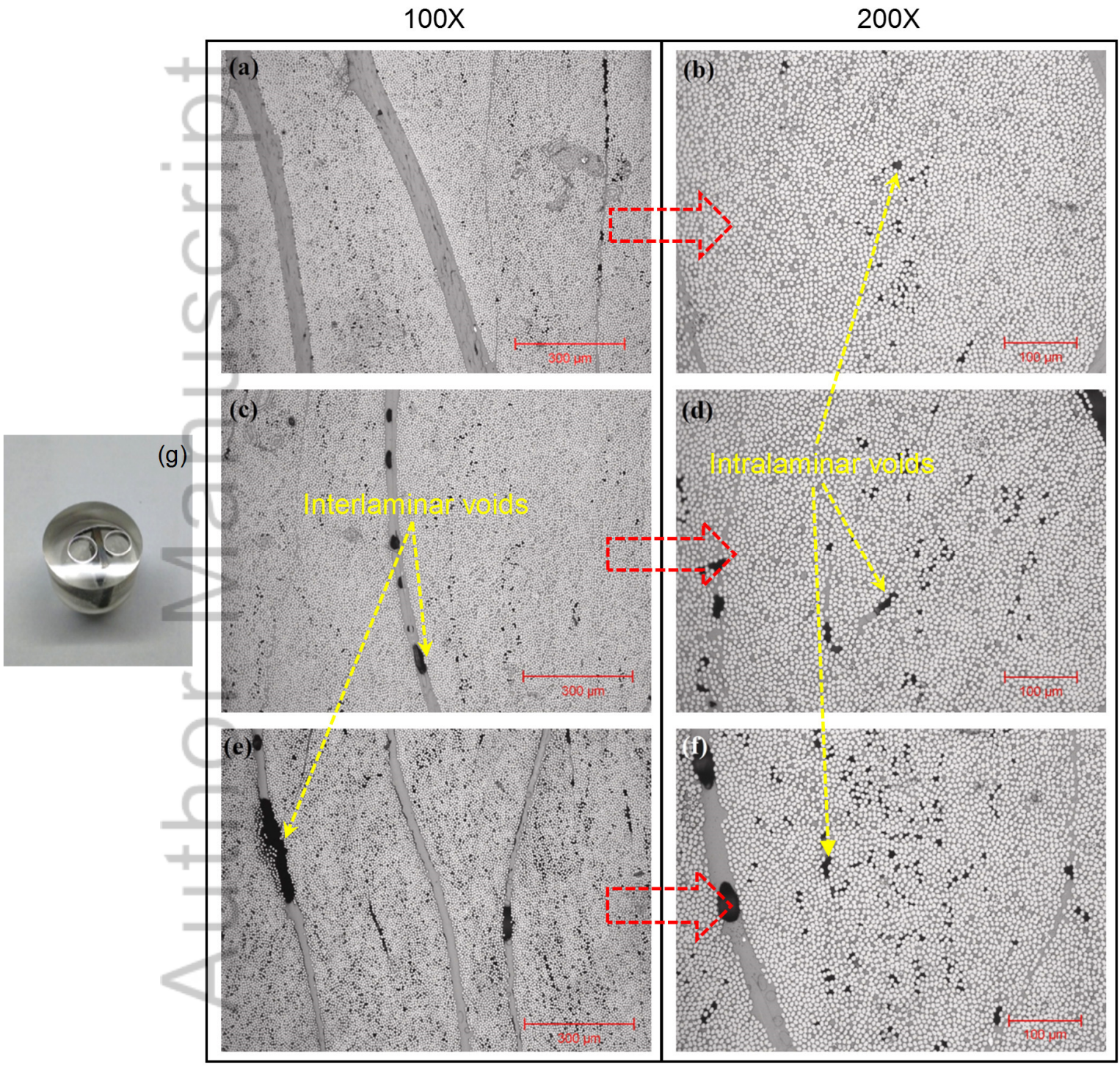

FFE_12721_F1.jpg

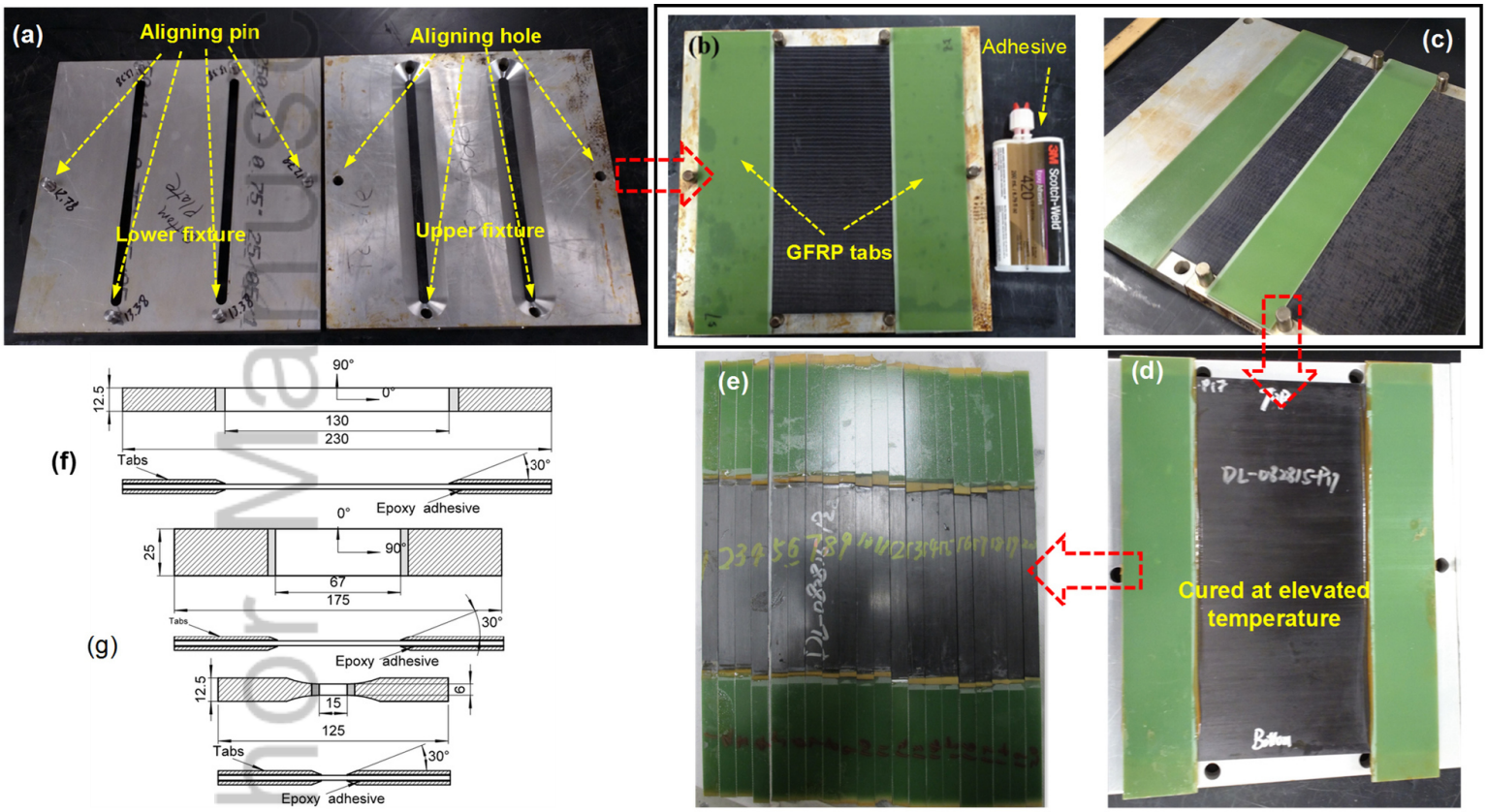

FFE_12721_F2.jpg

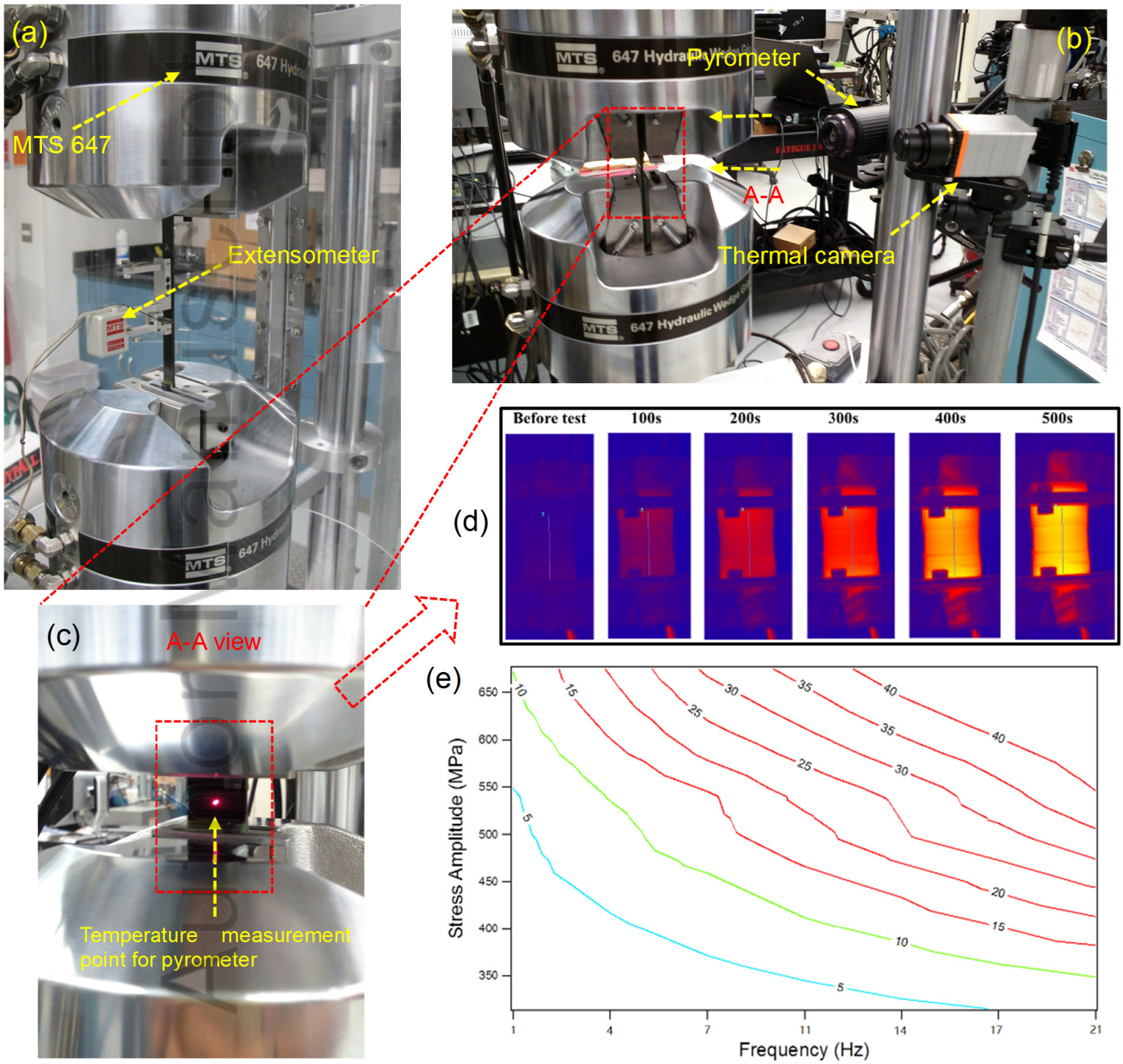

FFE_12721_F3.jpg

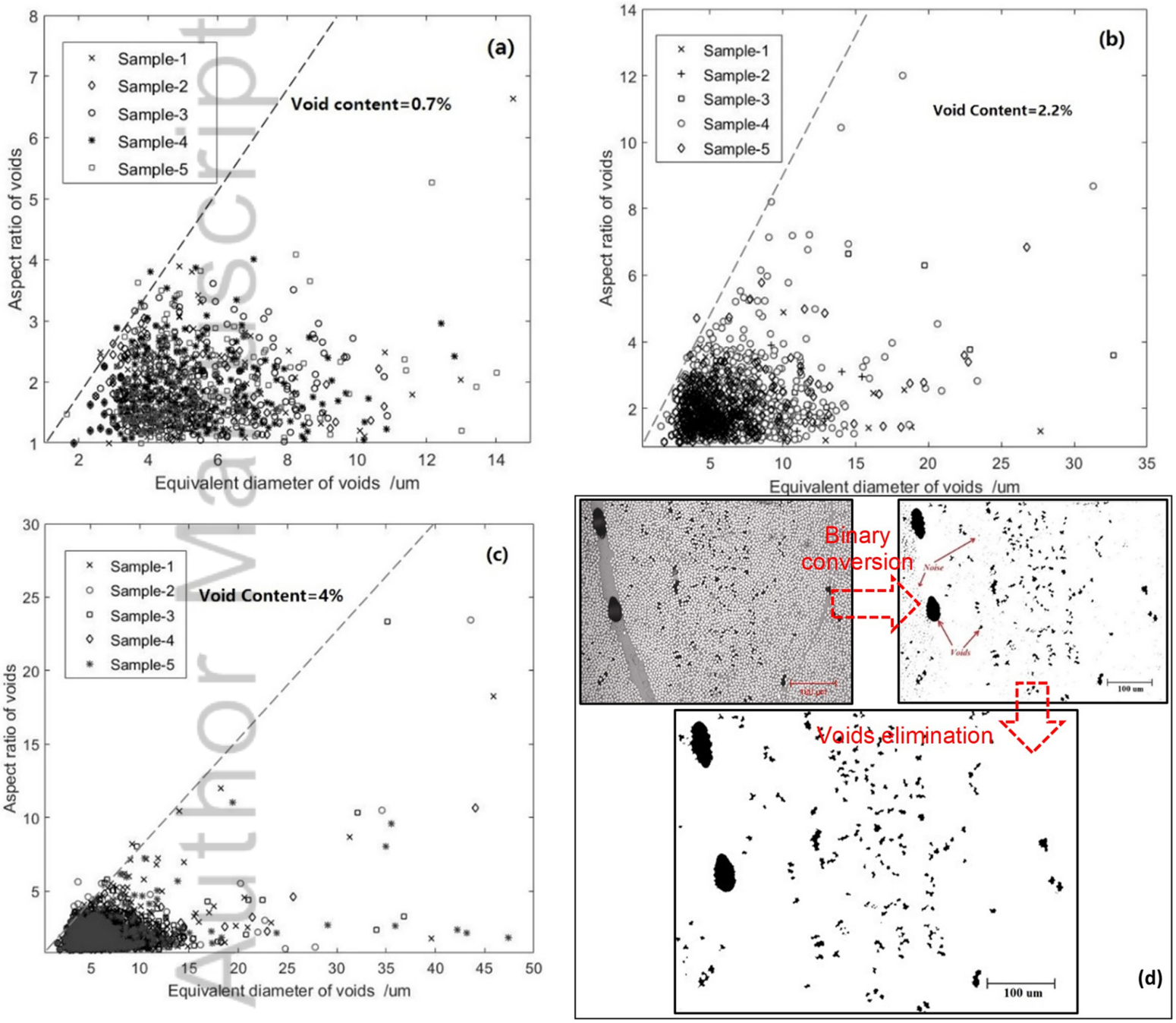

FFE_12721_F4.jpg

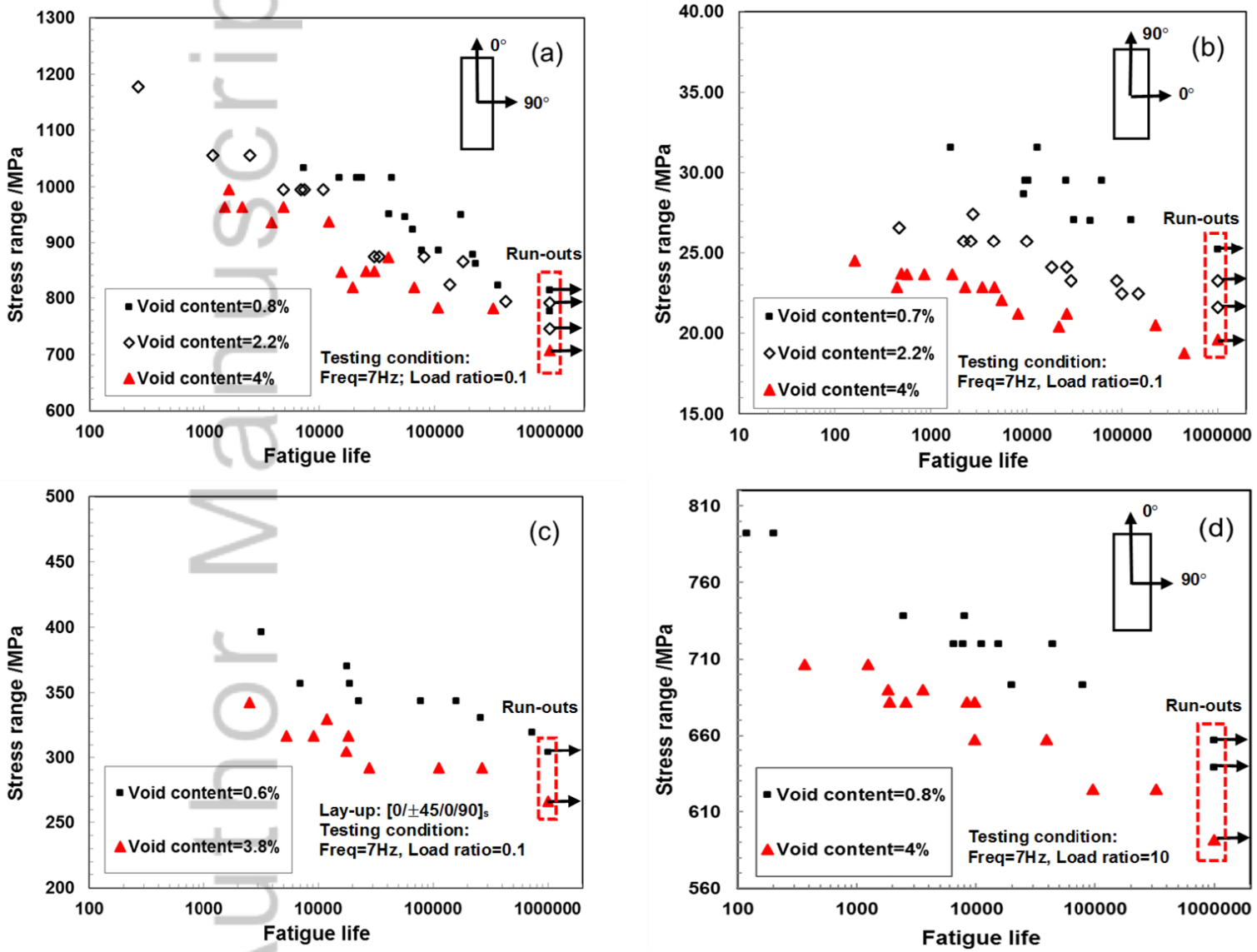

FFE_12721_F5.jpg

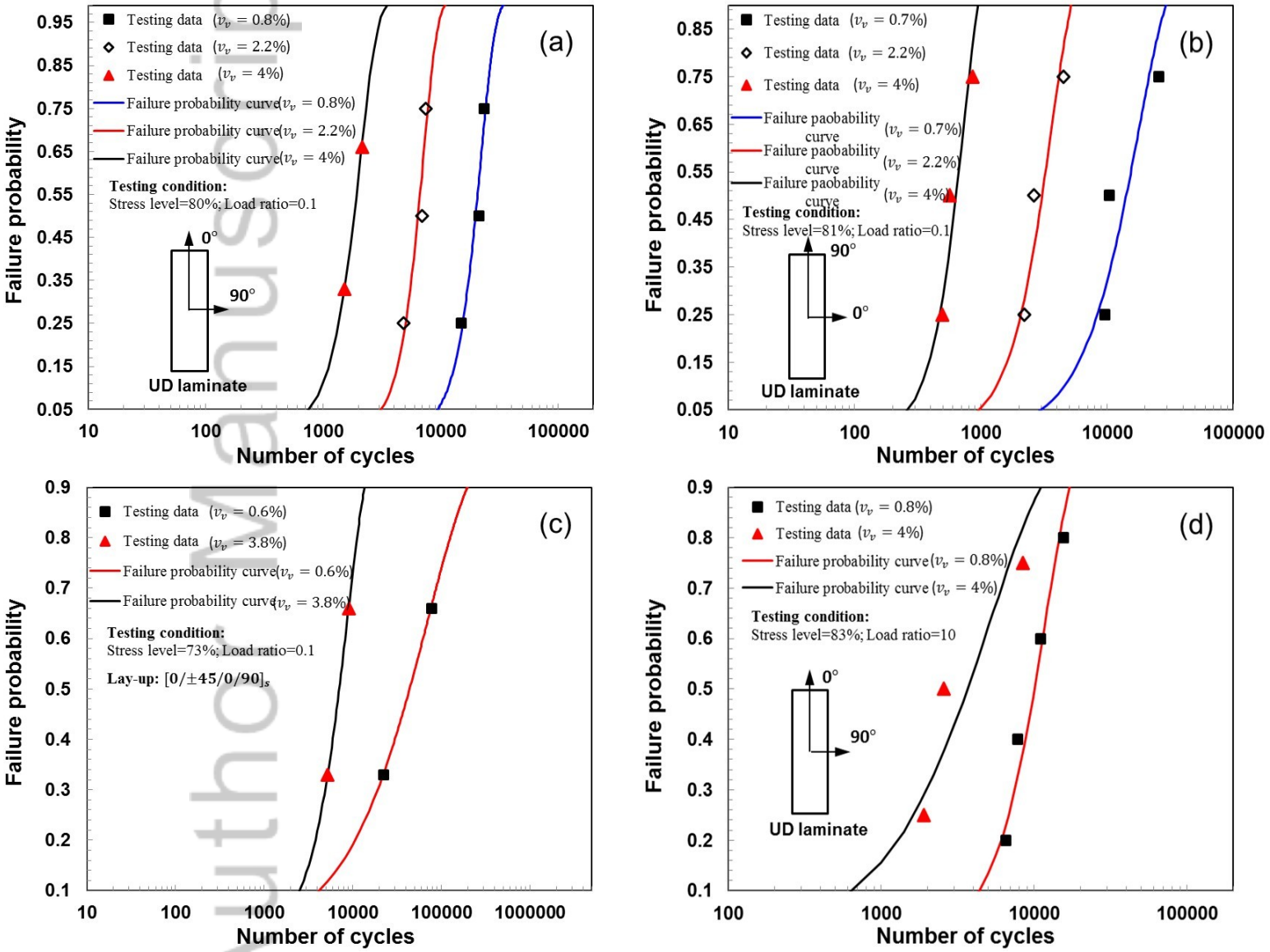

FFE_12721_F6.jpg

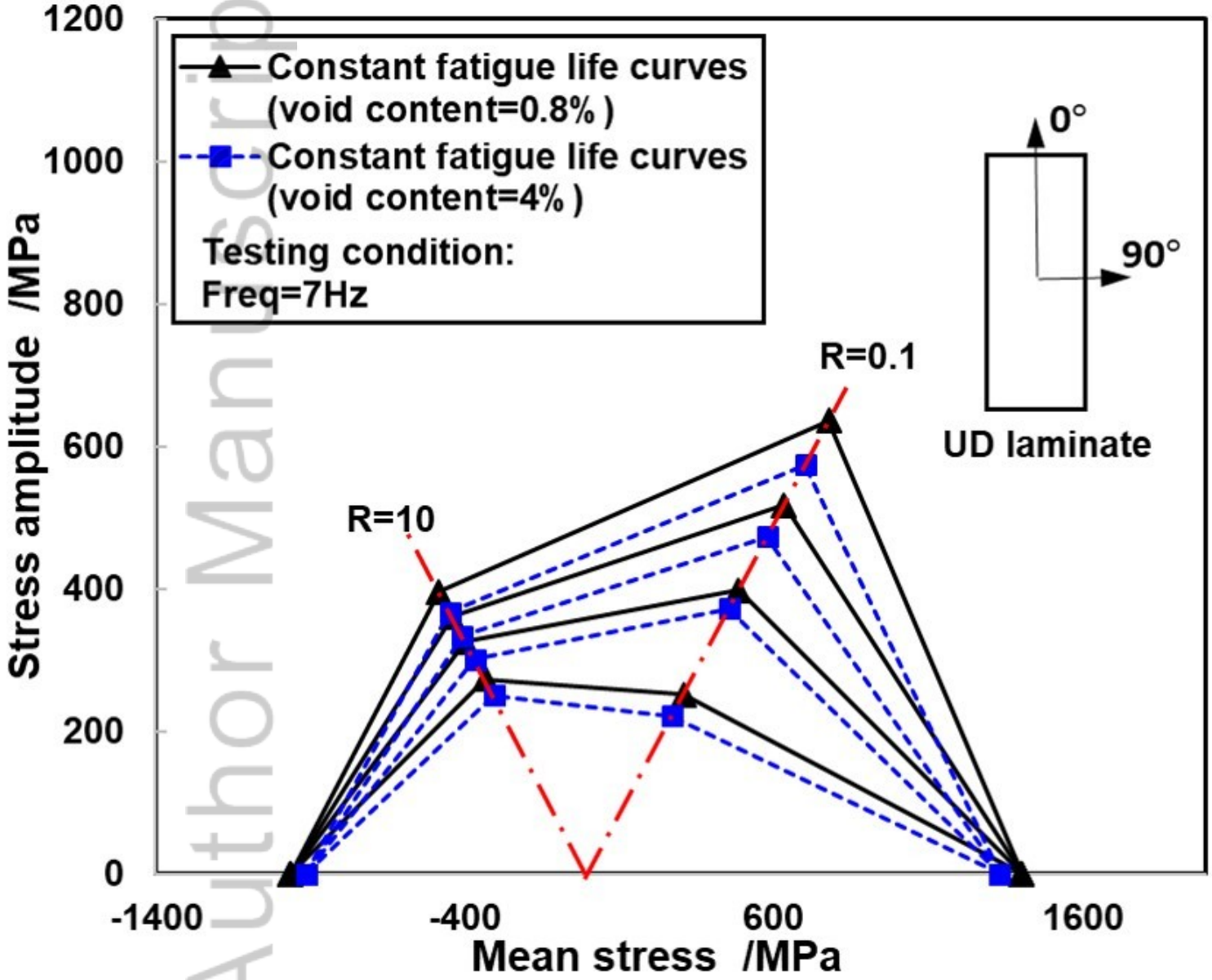

FFE_12721_F7.jpg

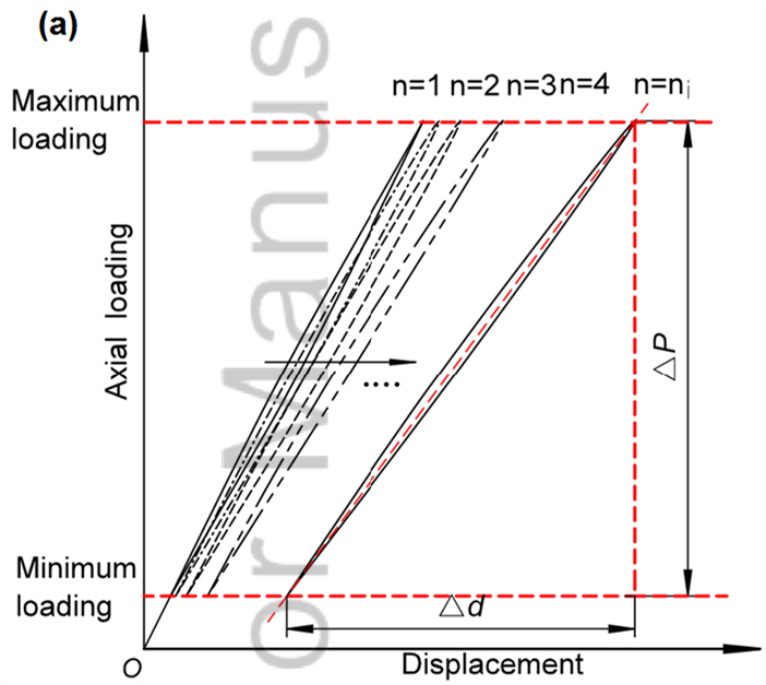

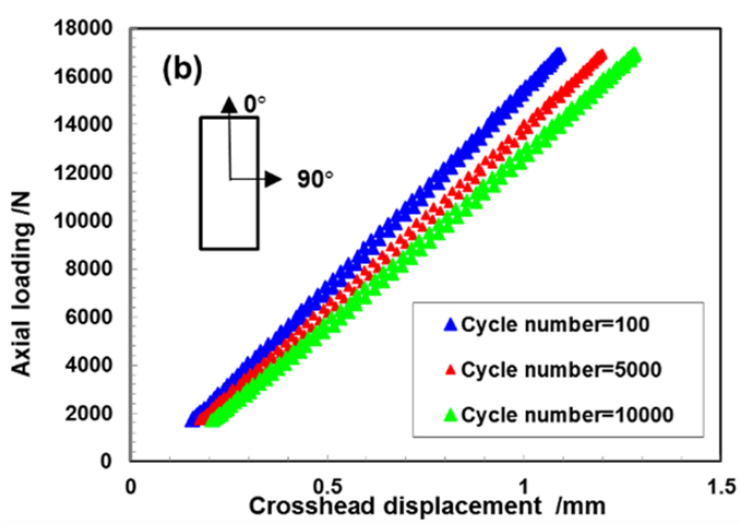

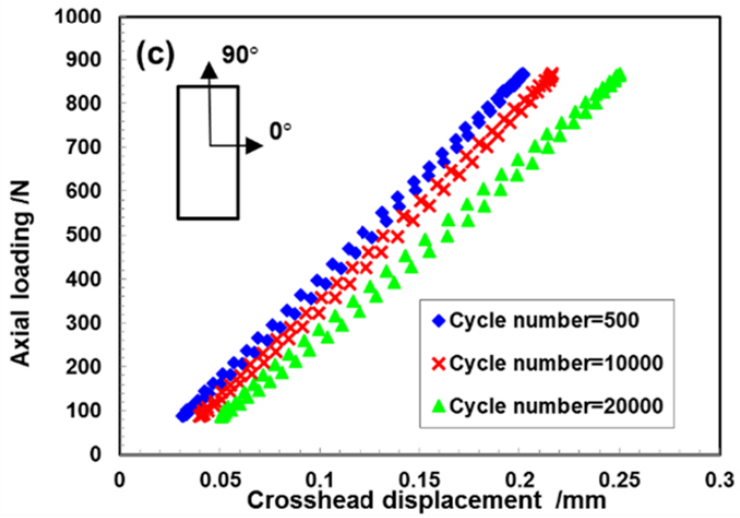

FFE_12721_F8.jpg

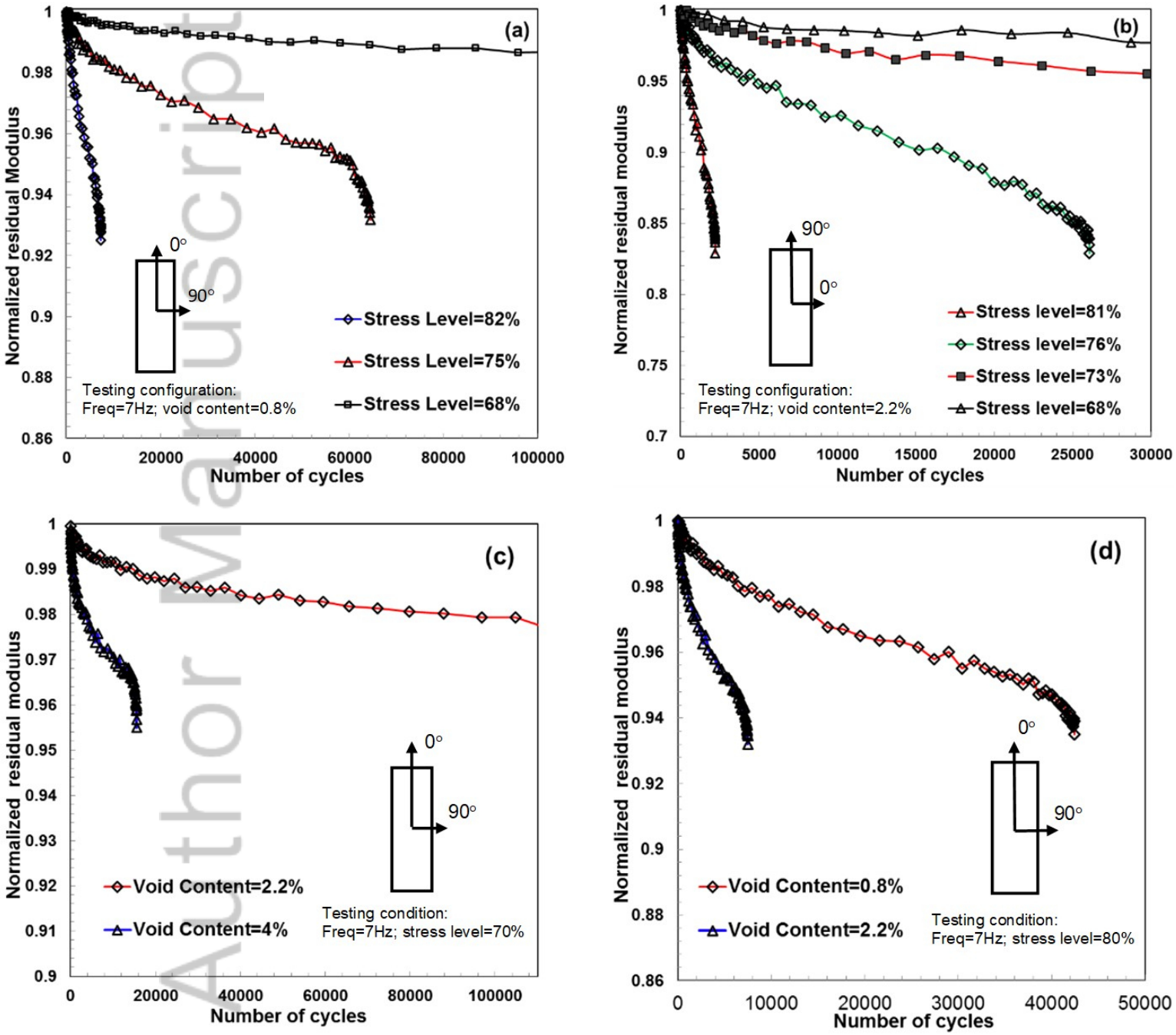

FFE_12721_F9.jpg

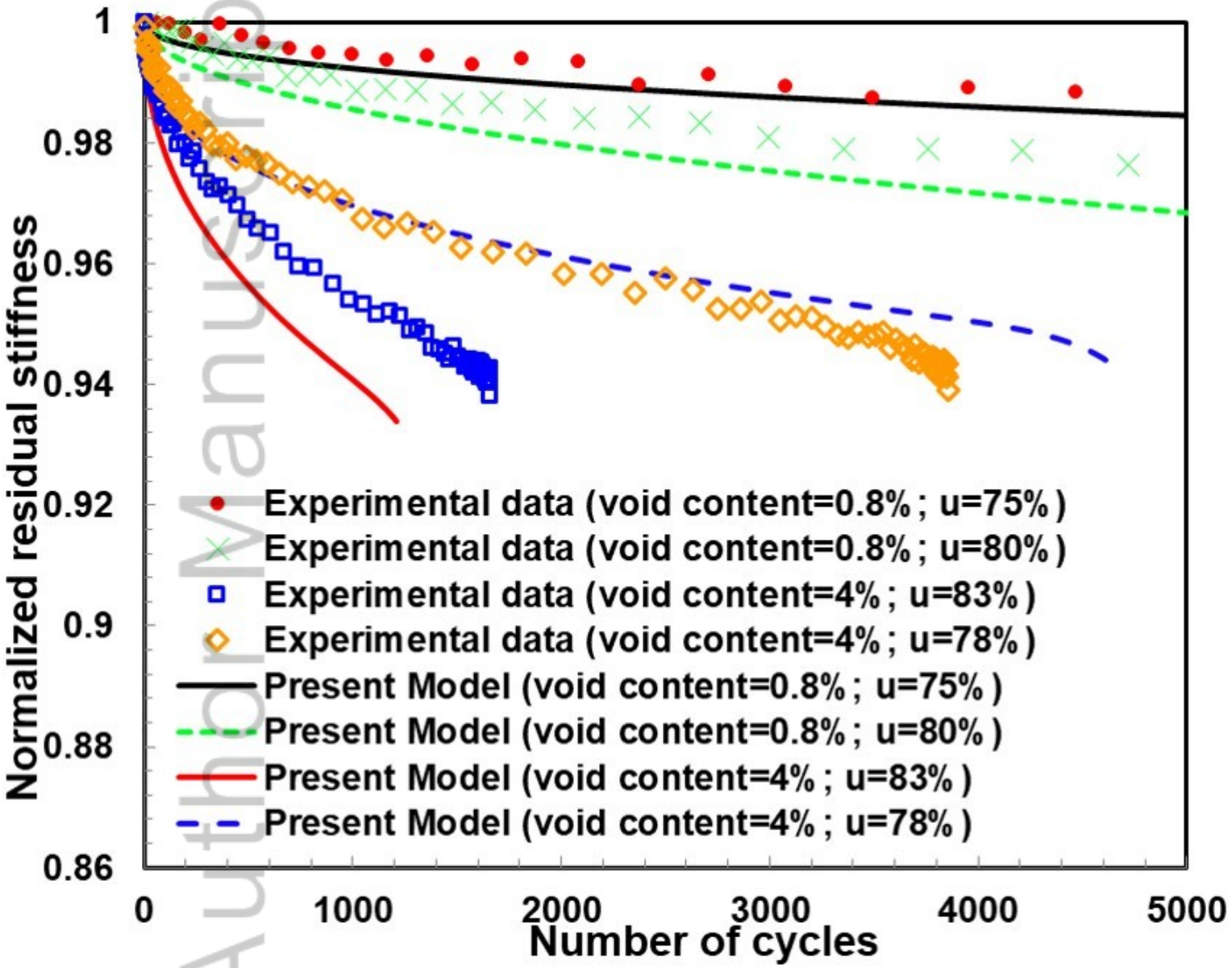

FFE_12721_F10.jpg

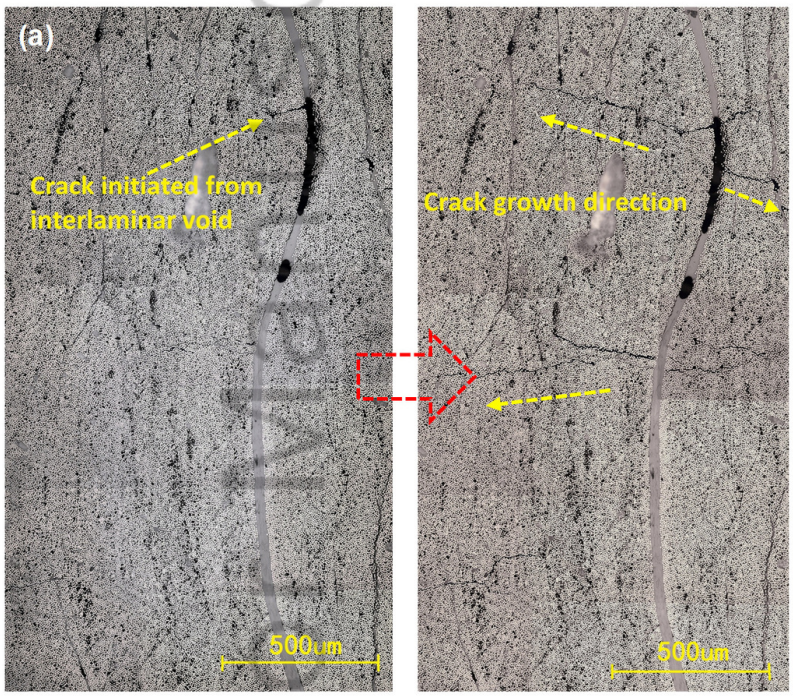

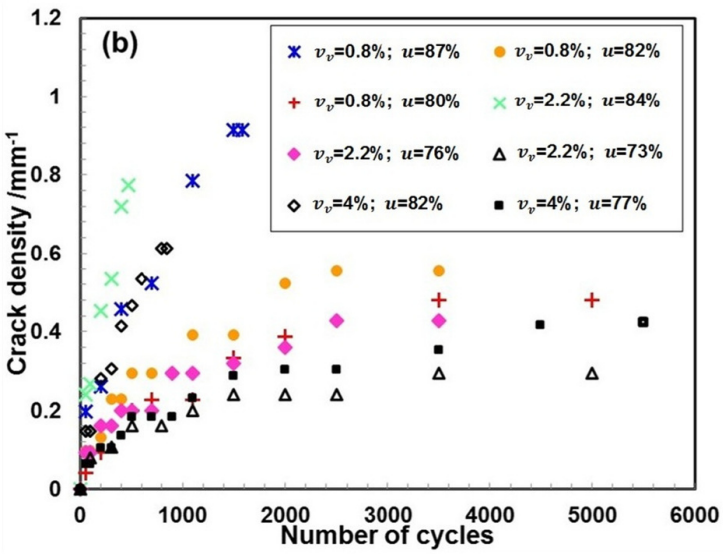

FFE_12721_F11.jpg

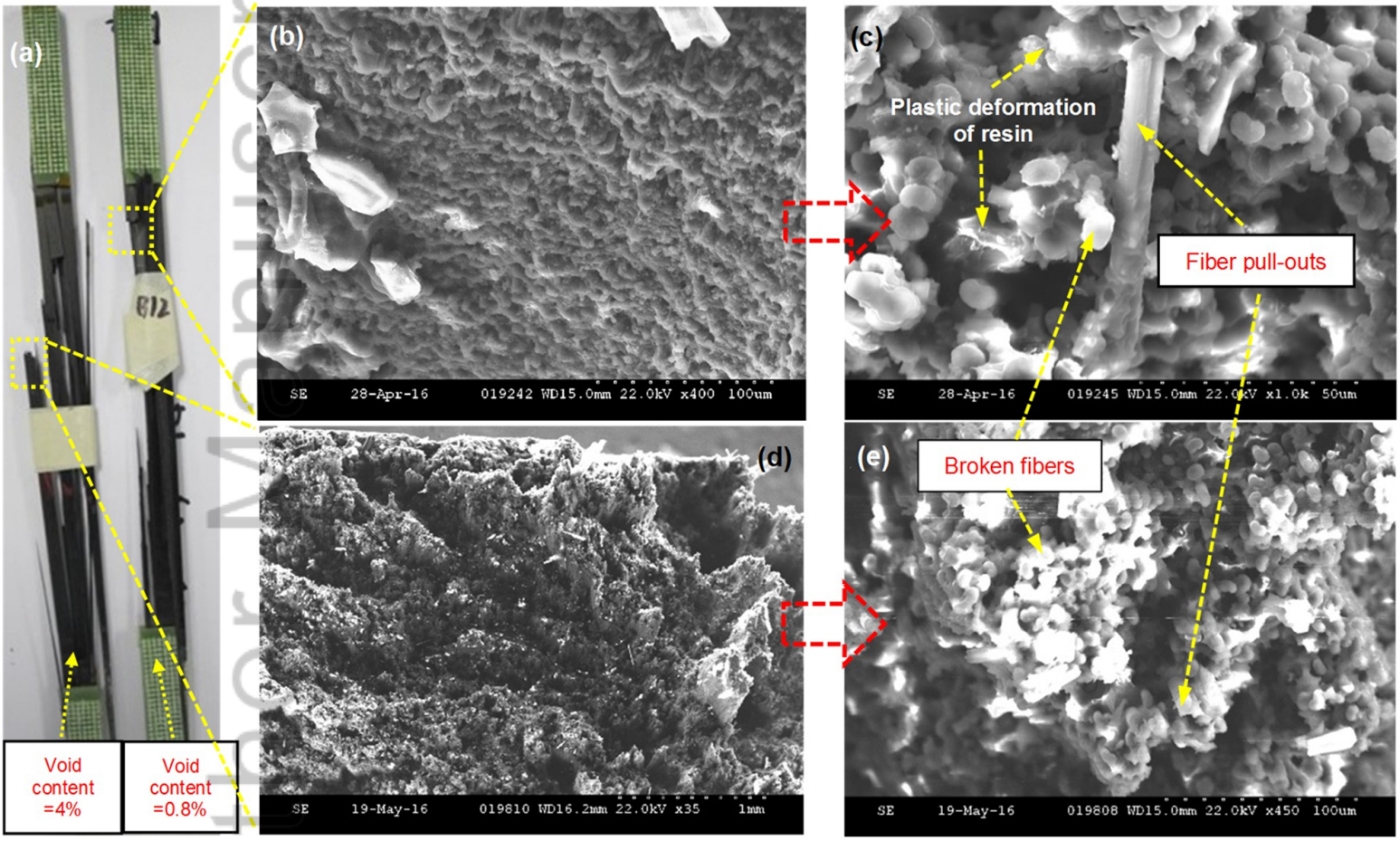

FFE_12721_F12.jpg

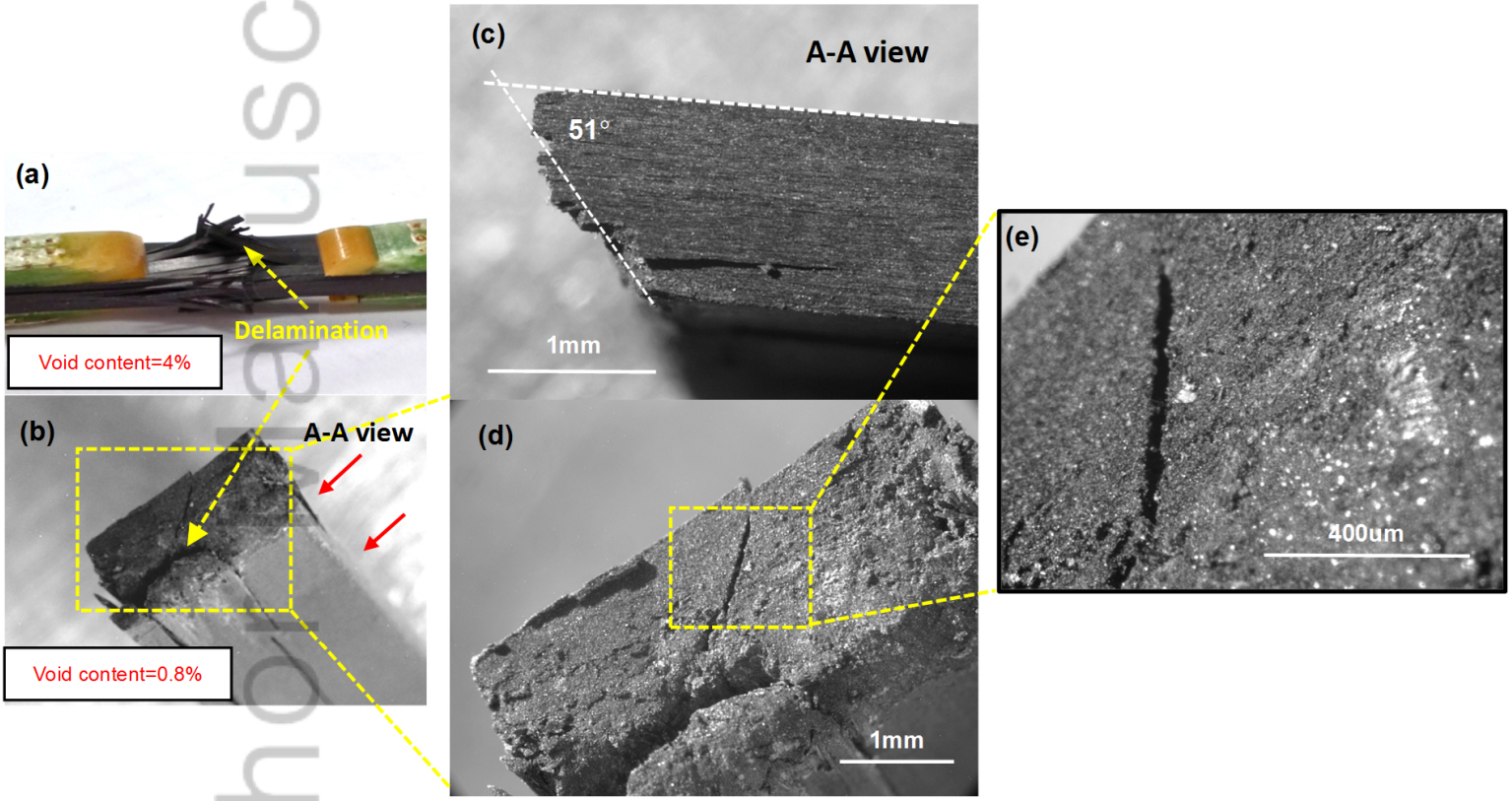

FFE_12721_F13.jpg

Liu Haolong (Orcid ID: 0000-0002-0762-2828)

Table 1. Void content of plaques cured under different compression pressures.

Panel #[a]	Sample lay-up	Compression pressure /MPa	Void content
UD-P16	$[0]_{16}$	0.5	0.8%
UD-P12A	$[90]_{12}$	0.5	0.7%
UD-P12B	$[0]_{12}$, $[90]_{12}$	0.3	2.2%
UD-P12C	$[0]_{12}$, $[90]_{12}$	0.1	4.0%
MD-PA	$[0/\pm45/0/90]_{s}$	0.5	0.6%
MD-PB	$[0/\pm45/0/90]_{s}$	0.1	3.8%

[a] UD=Unidirectional, MD=Multidirectional.

Liu Haolong (Orcid ID: 0000-0002-0762-2828)

Table 2. Fitting parameters of fatigue failure probability curve model.

Testing material	UD laminate (longitudinal)			UD laminate (transverse)			MD laminate $[0/\pm45/0/90]_s$		UD laminate (longitudinal)	
Stress ratio R	R=0.1								R=10	
Stress level u	80%			81%			73%		83%	
Void content	0.8%	2.2%	4%	0.7%	2.2%	4%	0.6%	3.8%	0.8%	4%
η	22026	7115	2071	17659	3594	720	69564	8639	11778	5115
λ	3.48	3.58	2.94	1.67	2.26	2.95	0.80	1.82	2.27	1.09